International Journal of Solids and Structures 45 (2008) 5205–5219

Contents lists available at ScienceDirect

International Journal of Solids and Structures

journal homepage: www.elsevier.com/locate/ijsolstr

An exact solution for the three-phase thermo-electro-magneto-elastic cylinder model and its application to piezoelectric–magnetic fiber composites

Z.H. Tong [a], S.H. Lo [b], C.P. Jiang [a], Y.K. Cheung [b,*]

[a] Solid mechanics Research Center, Beijing University of Aeronautics and Astronautics, Beijing 100083, China
[b] Department of Civil Engineering, The University of Hong Kong, Pokfulam Road, Hong Kong, China

ARTICLE INFO

Article history:
Received 26 October 2007
Received in revised form 10 March 2008
Available online 22 April 2008

Keywords:
Generalized self-consistent method
Eigenstrain
Piezoelectric–magnetic fiber composites
Thermo-electro-magnetic-elastic properties
Product properties

ABSTRACT

A three-phase cylindrical model for analyzing fiber composite subject to in-plane mechanical load under the coupling effects of multiple physical fields (thermo, electric, magnetic and elastic) is presented. By introducing an eigenstrain corresponding to the thermo-electro-magnetic-elastic effect, the complex multi-field coupling problem can be reduced to a formal in-plane elasticity problem for which an exact closed form solution is available. The present three-phase model can be applied to fiber/interphase/matrix composites, such that a lot of interesting thermo-electro-magnetism and stress coupling phenomena induced by the interphase layer are revealed. The present model can also be applied to fiber/matrix composites, in terms of which a generalized self-consistent method (GSCM) is developed for predicting the effective properties of piezoelectric–magnetic fiber reinforced composites. The effective piezoelectric, piezomagnetic, thermoelectric and magnetoelectric moduli can be expressed in compact explicit formulae for direct references and applications. A comparison of the predictions by the GSCM with available experimental data is presented, and interesting magnification effects and peculiar product properties are discussed. As a theoretical basis for the GSCM, the equivalence of the three sets of different average field equations in predicting the effective properties are proved, and this fact provides a strong evidence of mathematical rigor and physical realism in the formulation.

1. Introduction

Functional composite materials, such as piezoelectric, magnetostrictive and thermoelectroelastic composites have been rapidly developing with increasing applications in ultrasonic imaging devices, sensors, actuators and transducers etc. Such composites inherit the characteristics of functional materials, such as the piezoelectric and piezomagnetic properties which can be tailored to meet specific applications.

Some composite materials can provide superior properties compared to their mother monolithic constituent materials. Smith et al. (1985) and Shaulov et al. (1989) found that the piezocomposites can provide a higher piezoelectric strain modulus d_{31} than the constituents; Dunn (1993) numerical results showed that the effective thermal expansion coefficients of composites could significantly exceed those of the matrix and the fiber phases. An important application of composite structure is the use of the product property, which is found in the composite structures but is absent in the individual phases (Ryu et al., 2002). Van Suchtelen (1972) suggested that the combination of piezoelectric–piezomagnetic phases may exhibit a new

* Corresponding author. Tel.: +852 2859 2666; fax: +852 2559 5337.
E-mail address: hreccyk@hkucc.hku.hk (Y.K. Cheung).

0020-7683/$ - see front matter © 2008 Elsevier Ltd. All rights reserved.
doi:10.1016/j.ijsolstr.2008.04.003

material property – the magnetoelectric (ME) coupling effect (the product property). Van Run et al. (1974) reported that the fabrication of $BaTiO_3$–$CoFe_2O_4$ composite has a ME coefficient hundred times higher than that of Cr_2O_3 which was then one of the single-phase materials of the highest ME coefficient.

Inspired by the above interesting and exciting multi-field coupling phenomena as well as the excellent designability of composites including piezoelectric–magnetic fiber composites, scientists and engineers begin to pursue the optimal design for the desired applications. With the rapid advancement in technological research, it is expected that composites and completely novel materials could be conveniently designed and manufactured by direct engineering of their constituents. The traditional phenomenological approach, however, is of limited use in making prediction on the behaviours of new composite materials which have not come to exist yet. It requires that researches go beyond such phenomenology for a more comprehensive understanding of the interaction of microstructures and their thermo-electro-magneto-elastic coupling properties (Tadmor et al., 2000).

Micromechanics methods (for example, Hori and Nemat-Nasser, 1998) are useful tools to predict effective properties of composites. The dilute (Eshelby, 1957), self-consistent (Budiansky, 1965; Hill, 1965), differential (Mclaughlin, 1977) and Mori–Tanaka methods (Mori and Tanaka, 1973; Benveniste, 1987) are based on the two-phase micromechanics models that have been extensively used. In order to extend the two-phase model to the multi-field coupled composite structure, the coupled Eshelby's tensor analogs to the elasticity has been developed. Deeg (1980) and Wang (1992) presented the tensor solution of a piezoelectric ellipsoidal inclusion embedded in an infinite medium. Dunn and Taya (1993) simplified the piezoelectric Eshelby's tensors of the elliptic fiber problem and put them in explicit form instead of the elliptic integrals, and then they extended the dilute, self-consistent, Mori–Tanaka and differential micromechanics methods to cover piezoelectric composites. As for the piezomagnetic materials, Nan (1994, 1997) proposed a model to determine the coupled ME effect and coupled local fields of composites based on the Greens' function method and perturbation theory developed for piezoelectric composites. Huang and Kuo (1997) directly extended the Eshelby type equivalent inclusion method to piezomagnetic composites which is originally developed for piezoelectric composites by Dunn and Taya (1993), and they proposal the analogous simplification on Eshelby's tensors (Huang, 1998). The thermal expansion is another important coupled field problem. Similarly, many researchers have extended the classical two-phase models to thermoelectroelastic composites (Dunn, 1993; Budiansky, 1965, etc.). Using the method of effective field, Sevostianov et al. (2001) derived the electroelastic constants of piezocomposites, and Levin and Luchaninov (2001) further considered the thermo-piezoelectric matrix composites. They presented explicit expressions for the effective pyroelectric, dielectric, piezoelectric, elastic and thermoelastic constants of such composites.

The generalized self-consistent method (GSCM) is a more sophisticated micromechanics approach, which is based on the three-phase model of inclusion/matrix/composite. The method was originally developed by Kerner (1956) and could be regarded as an extension of the composite cylinder/sphere model (Hashin, 1962; Hashin and Rosen, 1964). The boundary conditions of the GSCM model are simpler and more reasonable compared to the composite cylinder/sphere model. However, the GSCM may increase the complexity of the solution process, and Smith (1974) and Christensen and Lo (1979) took a long journey to arrive at the correct solutions. It is shown that the GSCM possesses the mathematical rigor in their elasticity formulation and physical realism (Christensen, 1998). Comparisons between the GSCM and other micromechanics methods also reveal that the GSCM predictions exhibit the best agreement with experiment results (Christensen, 1990). Luo and Weng (1987) proposed a modified Mori–Tanaka method which is based on the three-phase model instead of the Eshelby's problem. As for thermo-electro-magneto-elastic composites, Grekov et al. (1989) studied the composite cylinder model for piezocomposites, and Benveniste (1995) gave the predictions of the ME coefficient, which is based on the composite cylinder model and the theory of exact connections of multi-fields. Jiang and Cheung (2001) presented a three-phase piezoelectric cylinder model. The model was applied to fiber/interphase/matrix composites, whereby the effect of the interphase layer was studied. Jiang et al. (2001) also presented a three-phase confocal elliptical model, in which the GSCM for piezocomposites was developed, and Sudak (2003) studied the effect of an interphase layer on the electroelastic stresses within a three-phase elliptic inclusion by using this model. To our best knowledge, the researches on the three-phase model are limited to a simple case of antiplane shear coupled with inplane electric load. So far, no report has been found for a three-phase model under inplane mechanical load coupling with thermo-electro-magnetical loads. For such a problem, multi-field coupling leads to a set of rather complicated differential equations. To overcome the mathematical difficulties, in this paper, an eigenstrain corresponding to the thermo-electro-magnetic fields is introduced. As a result, the multi-field coupled problem is reduced to an equivalent inplane elasticity problem, for which the mathematical manipulation is greatly simplified and a compact solution in closed form is available.

This paper is organized as follows. Section 2 establishes the three-phase model and introduces the eigenstrain to simplify the constitutive equations. Section 3 provides a solution in closed form for the elasticity inplane problem with an eigenstrain by the complex variable method. Section 4 deals with stress concentrations under thermo-electro-magneto-mechanical coupling loads. The full thermo-electro-magneto-elastic moduli are obtained in compact explicit form in Section 5, and through numerical examples, interesting coupling phenomena such as the abnormal magnification effect and the product effect for ME composites are discussed. In the appendix, the equivalence of three sets of different average field equations in predicting the effective properties by the GSCM is proved. They are: (1) the averaged stress in the representative volume element (RVE) is equal to the far-field one; (2) the averaged strain in the RVE is equal to the far-field one; (3) the averaged stress and strain in RVE satisfy the stress-strain relationship of the composite with the as-yet unknown effective properties.

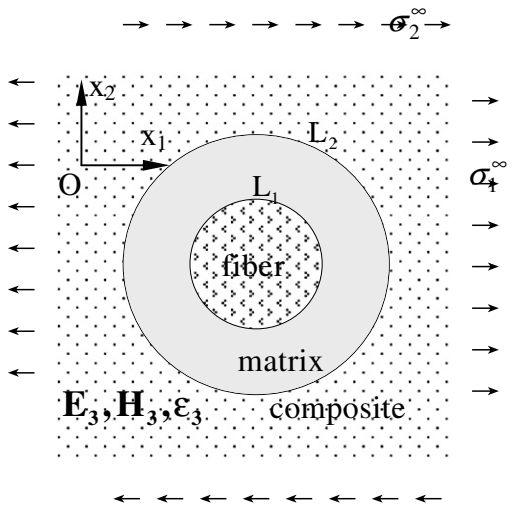

Fig. 1. Schematic diagram of the three-phase model cross-section.

2. Model and basic formulation

2.1. Three-phase model

Fig. 1 is a schematic diagram of a cross-section of the three-phase model, where the representative volume element (RVE) is composed of a circular fiber and a concentric circular matrix annulus with the same volume fraction λ as in the composite, which in turn is embedded in the infinite composite possessing the yet-unknown effective properties. Without losing generality, the outer radius of the matrix annulus is assumed to be 1, and then the radius of the fiber will be $\sqrt{\lambda}$. The poling direction of the materials is along x_3-direction (perpendicular to the paper) and the cross-section $Ox_1\,x_2$ is the transversely isotropic plane for each phase. Let the model be subjected to the far-field uniform stresses σ_1^∞ and σ_2^∞, along x_1- and x_2-directions, respectively. In the x_3-direction, there are a uniform strain ε_3, a uniform electrical field $E_{\mathbf{3}}$ and a uniform magnetic field $H_{\mathbf{3}}$. In the whole model a uniform thermal field θ is assumed.

2.2. Constitutive equations

The constitutive equations for a thermo-electro-magneto-elastic material under consideration are given by Benveniste (1995)

$$\begin{aligned}\boldsymbol{\sigma} &= \mathbf{C}\boldsymbol{\varepsilon} - \mathbf{e}E_{\mathbf{3}} - \mathbf{q}H_{\mathbf{3}} - \boldsymbol{\beta}\theta \\ D_3 &= \mathbf{e}^{\mathrm{T}}\boldsymbol{\varepsilon} + k_{33}E_{\mathbf{3}} + \alpha_{33}H_{\mathbf{3}} + p_3\theta \\ B_3 &= \mathbf{q}^{\mathrm{T}}\boldsymbol{\varepsilon} + \alpha_{33}E_{\mathbf{3}} + \mu_{33}H_{\mathbf{3}} + m_3\theta\end{aligned} \tag{1}$$

The stress–strain equation coupled with the thermo-electro-magnetic fields can also be expressed as

$$\boldsymbol{\varepsilon} = \mathbf{S}\boldsymbol{\sigma} + \mathbf{d}E_{\mathbf{3}} + \mathbf{g}H_{\mathbf{3}} + \boldsymbol{\rho}\theta \tag{2}$$

where $\boldsymbol{\sigma}$, $\boldsymbol{\varepsilon}$, D_3, B_3 are, respectively, the stress tensor, strain tensor, electric displacement and magnetic flux; $E_{\mathbf{3}}$, $H_{\mathbf{3}}$, θ are, respectively, the electric field intensity, the magnetic field intensity and the temperature change of the material; $\mathbf{C}$ denotes the stiffness matrix, $\mathbf{e}$, $\mathbf{q}$, $\boldsymbol{\beta}$ denote, respectively, the piezoelectric, piezomagnetic and thermal stress vectors; $\mathbf{S}$, $\mathbf{d}$, $\mathbf{g}$, $\boldsymbol{\rho}$, respectively, denote the material constants in the strain–stress equations which are corresponding to $\mathbf{C}$, $\mathbf{e}$, $\mathbf{q}$, $\boldsymbol{\beta}$ in the stress–strain equations; k_{33}, μ_{33} denote the dielectric constant and magnetic permeability; α_{33}, p_3, m_3 denote, respectively, the magneto-electric, pyroelectric and pyromagnetic coefficients.

For a transversely isotropic material, the above-mentioned vectors and matrices in expanded form can be written as

$$\begin{aligned}&\boldsymbol{\sigma} = \begin{bmatrix}\sigma_1\\ \sigma_2\\ \sigma_3\end{bmatrix} = \begin{bmatrix}\sigma_{11}\\ \sigma_{22}\\ \sigma_{33}\end{bmatrix}, \quad \boldsymbol{\varepsilon} = \begin{bmatrix}\varepsilon_1\\ \varepsilon_2\\ \varepsilon_3\end{bmatrix} = \begin{bmatrix}\varepsilon_{11}\\ \varepsilon_{22}\\ \varepsilon_{33}\end{bmatrix}, \quad \mathbf{C} = \begin{bmatrix}C_{11} & C_{12} & C_{13}\\ C_{12} & C_{11} & C_{13}\\ C_{13} & C_{13} & C_{33}\end{bmatrix} = \mathbf{S}^{-1} = \begin{pmatrix}\frac{1}{Y_1} & -\frac{\nu_{12}}{Y_1} & -\frac{\nu_{13}}{Y_3}\\ & \frac{1}{Y_1} & -\frac{\nu_{13}}{Y_3}\\ \text{sym} & & \frac{1}{Y_3}\end{pmatrix}^{-1}\\ &\mathbf{e} = \begin{pmatrix}e_{31}\\ e_{31}\\ e_{33}\end{pmatrix}, \quad \mathbf{q} = \begin{pmatrix}q_{31}\\ q_{31}\\ q_{33}\end{pmatrix}, \quad \boldsymbol{\beta} = \begin{pmatrix}\beta_1\\ \beta_1\\ \beta_3\end{pmatrix}, \quad \mathbf{d} = \begin{pmatrix}d_{31}\\ d_{31}\\ d_{33}\end{pmatrix}, \quad \mathbf{g} = \begin{pmatrix}g_{31}\\ g_{31}\\ g_{33}\end{pmatrix}, \quad \boldsymbol{\rho} = \begin{pmatrix}\rho_1\\ \rho_1\\ \rho_3\end{pmatrix}\end{aligned} \tag{3}$$

For the convenience of analysis, the longitudinal Young's modulus Y_3, the major Poisson's ratio v_{13}, as well as the transverse bulk modulus K and shear modulus μ are adopted. K, μ and the transverse Young's modulus Y_1, Poisson's ratio v_{12} can be converted by

$$\begin{aligned}&\left(\frac{1}{2K},\frac{1}{2\mu}\right)=\left(\frac{1-v_{12}}{Y_1}-\frac{2v_{13}^2}{Y_3},\frac{1+v_{12}}{Y_1}\right)\\&\left(\frac{1}{Y_1},v_{12}\right)=\left(\frac{1}{4K}+\frac{1}{4\mu}+\frac{v_{13}^2}{Y_3},\frac{-\frac{1}{K}+\frac{1}{\mu}-\frac{4v_{13}^2}{Y_3}}{\frac{1}{K}+\frac{1}{\mu}+\frac{4v_{13}^2}{Y_3}}\right)\end{aligned}\tag{4}$$

K, μ, v_{13}, Y_3 can also be expressed by C_{11}, C_{12}, C_{13}, C_{33} as

$$K=\frac{C_{11}+C_{12}}{2},\quad \mu=\frac{C_{11}-C_{12}}{2},\quad v_{13}=\frac{C_{13}}{C_{11}+C_{12}},\quad Y_3=C_{33}-\frac{2C_{13}^2}{C_{11}+C_{12}}\tag{5}$$

The coupled stress moduli and strain moduli can be converted by using the elastic stiffness matrix or the compliance matrix, that is

$$(\mathbf{d},\mathbf{g},\boldsymbol{\rho})=\mathbf{S}\bullet(\mathbf{e},\mathbf{q},\boldsymbol{\beta})\quad\text{or}\quad(\mathbf{e},\mathbf{q},\boldsymbol{\beta})=\mathbf{C}\bullet(\mathbf{d},\mathbf{g},\boldsymbol{\rho})\tag{6}$$

The above equations in expanded form are as follows

$$\begin{aligned}&\begin{bmatrix}d_{31}&g_{31}&\rho_1\\d_{33}&g_{33}&\rho_3\end{bmatrix}=\begin{bmatrix}\frac{1}{2K}+\frac{2v_{13}^2}{Y_3}&-\frac{v_{13}}{Y_3}\\-\frac{2v_{13}}{Y_3}&\frac{1}{Y_3}\end{bmatrix}\begin{bmatrix}e_{31}&q_{31}&\beta_1\\e_{33}&q_{33}&\beta_3\end{bmatrix}\\&\begin{bmatrix}e_{31}&q_{31}&\beta_1\\e_{33}&q_{33}&\beta_3\end{bmatrix}=\begin{bmatrix}2K&2v_{13}K\\4v_{13}K&(Y_3+4v_{13}^2K)\end{bmatrix}\begin{bmatrix}d_{31}&g_{31}&\rho_1\\d_{33}&g_{33}&\rho_3\end{bmatrix}.\end{aligned}\tag{7}$$

2.3. Eigenstrain equivalent medium concept

The constitutive Eq. (1) or (2) are rather complicated. However, it is observed that ε_3, E_3, H_3 and θ are constants in the whole model. The equivalent medium concept can be used to reduce the multi-field problem to an equivalent elastic one. Introduce a suitable uniform eigenstrain field ε^* in the transverse plane

$$\varepsilon_1^*=\varepsilon_2^*=\varepsilon^*=-v_{13}\varepsilon_{\mathbf{3}}+\frac{e_{31}}{2K}E_{\mathbf{3}}+\frac{q_{31}}{2K}H_{\mathbf{3}}+\frac{\beta_1}{2K}\theta\tag{8}$$

Then the constitutive Eq. (1) are simplified to

$$\begin{aligned}&(\sigma_1+\sigma_2)=2K(\varepsilon_1+\varepsilon_2-2\varepsilon^*),\quad(\sigma_2-\sigma_1)=2\mu(\varepsilon_2-\varepsilon_1)\\&\sigma_3=2v_{13}K(\varepsilon_1+\varepsilon_2)+(4Kv_{13}^2+Y_3)\varepsilon_3-e_{33}E_3-q_{33}H_3-\beta_3\theta\\&D_3=e_{31}(\varepsilon_1+\varepsilon_2)+e_{33}\varepsilon_3+k_{33}E_{\mathbf{3}}+\alpha_{33}H_{\mathbf{3}}+p_3\theta\\&B_3=q_{31}(\varepsilon_1+\varepsilon_2)+q_{33}\varepsilon_3+\alpha_{33}E_{\mathbf{3}}+\mu_{33}H_{\mathbf{3}}+m_3\theta\end{aligned}\tag{9}$$

It is seen that the stress–strain field in a thermo-electro-magneto-elastic material is the same as that in the corresponding elastic material with a suitable uniform eigenstrain field ε^*. Thus the multi-field coupled problem is reduced to an equivalent inplane elastic problem with a suitable eigenstrain. Similarly, the problem can also be studied by introducing an eigenstress.

3. Complex variable solution

3.1. Complex variable method

According to Muskhelishivili (1965), an inplane elastic problem can be formulated by two complex potentials $\varphi(z)$ and $\psi(z)$, in terms of which, the stresses σ_1, σ_2, σ_{12} are expressed by

$$\begin{aligned}&\sigma_1+\sigma_2=4\mathrm{Re}[\varphi'(z)]\\&\sigma_2-\sigma_1+2\mathrm{i}\sigma_{12}=2[\bar{z}\varphi''(z)+\psi'(z)]\end{aligned}\tag{10}$$

where the overbar represents the complex conjugate, the prime denotes differentiation. The displacement and resultant stress components are then obtained as

$$\begin{aligned}&(u_1+\mathrm{i}u_2)=\frac{1}{2\mu}[\kappa\varphi(z)-\overline{\omega(z)}]+\varepsilon^*z\\&(F_1+\mathrm{i}F_2)=-\mathrm{i}[\varphi(z)+\overline{\omega(z)}]_{\mathrm{A}}^{\mathrm{B}}\end{aligned}\tag{11}$$

and

$$\begin{aligned}&\overline{\omega(z)} = z\overline{\varphi'(z)} + \overline{\psi(z)},\\ &\kappa = 1 + \frac{2\mu}{K}\end{aligned} \tag{12}$$

where u_1 and u_2 are, respectively, the displacement components along x_1- and x_2-axes, F_1 and F_2 are, respectively, the resultant stress components from point A to point B along any arc, and $[\bullet]_A^B$ means the value difference between two points A and B.

3.2. Stress and displacement continuity conditions on the interfaces

As shown in Fig. 1, L_1 and L_2 denote the interfaces between the fiber, matrix and equivalent composite medium, respectively. Assuming that the interfaces L_1 and L_2 are perfectly bonded, the continuity conditions of displacements and stresses can be expressed as (Jiang et al., 2003)

$$\begin{aligned}&(u_1 + \mathrm{i}u_2)_\mathrm{f} = (u + \mathrm{i}v)_\mathrm{m}, \quad (F_1 + \mathrm{i}F_2)_\mathrm{f} = (F_1 + \mathrm{i}F_2)_\mathrm{m}, \quad \text{on } L_1\\ &(u_1 + \mathrm{i}u_2)_\mathrm{m} = (u + \mathrm{i}v)_\mathrm{c}, \quad (F_1 + \mathrm{i}F_2)_\mathrm{m} = (F_1 + \mathrm{i}F_2)_\mathrm{c}, \quad \text{on } L_2\end{aligned} \tag{13}$$

where the subscripts f, m, c refer to the fiber, matrix and homogenized composite, respectively.

Introducing the following normalized parameters

$$\begin{aligned}&p_\mathrm{fm} = \frac{K_\mathrm{f}^{-1} - K_\mathrm{m}^{-1}}{K_\mathrm{m}^{-1} + \mu_\mathrm{m}^{-1}}, \quad q_\mathrm{fm} = \frac{\mu_\mathrm{f}^{-1} - \mu_\mathrm{m}^{-1}}{2(K_\mathrm{m}^{-1} + \mu_\mathrm{m}^{-1})}, \quad t_\mathrm{fm} = \frac{\varepsilon_\mathrm{f}^* - \varepsilon_\mathrm{m}^*}{K_\mathrm{m}^{-1} + \mu_\mathrm{m}^{-1}},\\ &p_\mathrm{cm} = \frac{K_\mathrm{c}^{-1} - K_\mathrm{m}^{-1}}{K_\mathrm{m}^{-1} + \mu_\mathrm{m}^{-1}}, \quad q_\mathrm{cm} = \frac{\mu_\mathrm{c}^{-1} - \mu_\mathrm{m}^{-1}}{2(K_\mathrm{m}^{-1} + \mu_\mathrm{m}^{-1})}, \quad t_\mathrm{cm} = \frac{\varepsilon_\mathrm{c}^* - \varepsilon_\mathrm{m}^*}{K_\mathrm{m}^{-1} + \mu_\mathrm{m}^{-1}}\end{aligned} \tag{14}$$

and noting Eq. (11), the continuity conditions (13) are then transformed as

$$\begin{aligned}&\varphi_\mathrm{m}(z) = (1 + p_\mathrm{fm} + q_\mathrm{fm})\varphi_\mathrm{f}(z) - q_\mathrm{fm}\overline{\omega_\mathrm{f}(z)} + t_\mathrm{fm}z\\ &\overline{\omega_\mathrm{m}(z)} = -(p_\mathrm{fm} + q_\mathrm{fm})\varphi_\mathrm{f}(z) + (1 + q_\mathrm{fm})\overline{\omega_\mathrm{f}(z)} - t_\mathrm{fm}z, \quad r = \sqrt{\lambda}\\ &(1 + p_\mathrm{cm} + 2q_\mathrm{cm})\varphi_\mathrm{c}(z) = (1 + q_\mathrm{cm})\varphi_\mathrm{m}(z) + q_\mathrm{cm}\overline{\omega_\mathrm{m}(z)} - t_\mathrm{cm}z\\ &(1 + p_\mathrm{cm} + 2q_\mathrm{cm})\overline{\omega_\mathrm{c}(z)} = (p_\mathrm{cm} + q_\mathrm{cm})\varphi_\mathrm{m}(z) + (1 + p_\mathrm{cm} + q_\mathrm{cm})\overline{\omega_\mathrm{m}(z)} + t_\mathrm{cm}z, \quad r = 1\end{aligned} \tag{15}$$

where $r = \sqrt{\lambda}$ and $r = 1$ are the radii of L_1 and L_2, respectively.

3.3. Closed form solution

It is observed that a closed form solution of Eq. (15) can be achieved by taking the following finite series expansions of the complex potentials

$$\begin{aligned}&\varphi_\mathrm{f}(z) = a_1^\mathrm{f} z + a_3^\mathrm{f} z^3, \quad \psi_\mathrm{f}(z) = b_1^\mathrm{f} z;\\ &\varphi_\mathrm{m}(z) = a_1^\mathrm{m} z + a_3^\mathrm{m} z^3 + a_{-1}^\mathrm{m}\frac{1}{z}, \quad \psi_\mathrm{m}(z) = b_1^\mathrm{m} z + b_{-1}^\mathrm{m}\frac{1}{z} + b_{-3}^\mathrm{m}\frac{1}{z^3};\\ &\varphi_\mathrm{c}(z) = a_1^\mathrm{c} z + a_{-1}^\mathrm{c}\frac{1}{z}, \quad \psi_\mathrm{c}(z) = b_1^\mathrm{c} z + b_{-1}^\mathrm{c}\frac{1}{z} + b_{-3}^\mathrm{c}\frac{1}{z^3}\end{aligned} \tag{16}$$

where $a_1^\mathrm{f}, a_3^\mathrm{f}, b_1^\mathrm{f}, a_1^\mathrm{m}, a_3^\mathrm{m}, a_{-1}^\mathrm{m}, b_1^\mathrm{m}, b_{-1}^\mathrm{m}, b_{-3}^\mathrm{m}, a_1^\mathrm{c}, a_{-1}^\mathrm{c}, b_1^\mathrm{c}, b_{-1}^\mathrm{c}, b_{-3}^\mathrm{c}$ are real coefficients.

Substituting Eq. (16) into Eq. (12), we have

$$\begin{aligned}&\overline{\omega_\mathrm{f}(z)} = a_1^\mathrm{f} z + (3r^4 a_3^\mathrm{f} + r^2 b_1^\mathrm{f})\frac{1}{z},\\ &\overline{\omega_\mathrm{m}(z)} = \left(a_1^\mathrm{m} + \frac{b_{-1}^\mathrm{m}}{r^2}\right)z + (3r^4 a_3^\mathrm{m} + r^2 b_1^\mathrm{m})\frac{1}{z} + \left(-\frac{a_{-1}^\mathrm{m}}{r^4} + \frac{b_{-3}^\mathrm{m}}{r^6}\right)z^3,\\ &\overline{\omega_\mathrm{c}(z)} = \left(a_1^\mathrm{c} + \frac{b_{-1}^\mathrm{c}}{r^2}\right)z + r^2 b_1^\mathrm{c}\frac{1}{z} + \left(-\frac{a_{-1}^\mathrm{c}}{r^4} + \frac{b_{-3}^\mathrm{c}}{r^6}\right)z^3\end{aligned} \tag{17}$$

Letting $z \to \infty$, the far-field conditions give

$$a_1^{\mathrm{c}} = \frac{1}{4}(\sigma_1^{\infty} + \sigma_2^{\infty}), \quad b_1^{\mathrm{c}} = \frac{1}{2}(\sigma_2^{\infty} - \sigma_1^{\infty}) \tag{18}$$

Substituting Eqs. (16) and (17) to Eq. (15), noting $\bar{z} = r^2/z$ and comparing the coefficients of the same order of z, we obtain

$$\begin{aligned}
&a_1^{m} = (1 + p_{\mathrm{fm}} + q_{\mathrm{fm}})a_1^{\mathrm{f}} - q_{\mathrm{fm}}a_1^{\mathrm{f}} + t_{\mathrm{fm}} \\
&a_1^{\mathrm{m}} + \frac{b_{-1}^{\mathrm{m}}}{\lambda} = -(p_{\mathrm{fm}} + q_{\mathrm{fm}})a_1^{\mathrm{f}} + (1 + q_{\mathrm{fm}})a_1^{\mathrm{f}} - t_{\mathrm{fm}} \\
&a_3^{\mathrm{m}} = (1 + p_{\mathrm{fm}} + q_{\mathrm{fm}})a_3^{\mathrm{f}} \\
&a_{-1}^{\mathrm{m}} = -q_{\mathrm{fm}}(3a_3^{\mathrm{f}}\lambda^2 + b_1^{\mathrm{f}}\lambda) \\
&(3a_3^{\mathrm{m}}\lambda^2 + b_1^{\mathrm{m}}\lambda) = (1 + q_{\mathrm{fm}})(3a_3^{\mathrm{f}}\lambda^2 + b_1^{\mathrm{f}}\lambda) \\
&\left(-\frac{a_{-1}^{\mathrm{m}}}{\lambda^2} + \frac{b_{-3}^{\mathrm{m}}}{\lambda^3}\right) = -(p_{\mathrm{fm}} + q_{\mathrm{fm}})a_3^{\mathrm{f}} \\
&(1 + p_{\mathrm{cm}} + 2q_{\mathrm{cm}})a_1^{\mathrm{c}} = (1 + q_{\mathrm{cm}})a_1^{\mathrm{m}} + q_{\mathrm{cm}}(a_1^{\mathrm{m}} + b_{-1}^{\mathrm{m}}) - t_{\mathrm{cm}} \\
&0 = (1 + q_{\mathrm{cm}})a_3^{\mathrm{m}} + q_{\mathrm{cm}}(-a_{-1}^{\mathrm{m}} + b_{-3}^{\mathrm{m}}) \\
&(1 + p_{\mathrm{cm}} + 2q_{\mathrm{cm}})b_1^{\mathrm{c}} = (p_{\mathrm{cm}} + q_{\mathrm{cm}})a_{-1}^{\mathrm{m}} + (1 + p_{\mathrm{cm}} + q_{\mathrm{cm}})(3a_3^{\mathrm{m}} + b_1^{\mathrm{m}})
\end{aligned} \tag{19}$$

where the three equations on $a_{-1}^{\mathrm{c}}, b_{-1}^{\mathrm{c}}, b_{-3}^{\mathrm{c}}$ were not written as they will not be used. The coefficients can be obtained as follows

$$\begin{aligned}
&a_1^{\mathrm{f}} = \frac{(1+p_{\mathrm{cm}}+2q_{\mathrm{cm}})\frac{1}{4}(\sigma_1^{\infty}+\sigma_2^{\infty}) - [1+2(1-\lambda)q_{\mathrm{cm}}]t_{\mathrm{fm}} + t_{\mathrm{cm}}}{(1+p_{\mathrm{fm}}+2q_{\mathrm{cm}}) + 2(1-\lambda)p_{\mathrm{fm}}q_{\mathrm{cm}}} \\
&\begin{bmatrix} a_3^{\mathrm{f}} \\ b_1^{\mathrm{f}} \end{bmatrix} = (\mathbf{Q}_{\mathrm{mc}}\mathbf{Q}_{\mathrm{fm}})^{-1}\begin{bmatrix} 0 \\ 1 \end{bmatrix}\frac{1}{2}(\sigma_2^{\infty} - \sigma_1^{\infty})
\end{aligned} \tag{20}$$

$$\begin{bmatrix} a_1^{\mathrm{m}} \\ b_{-1}^{\mathrm{m}} \end{bmatrix} = \mathbf{P}_{\mathrm{fm}}a_1^{\mathrm{f}} + \mathbf{R}_{\mathrm{fm}}, \quad \begin{bmatrix} a_3^{\mathrm{m}} \\ a_{-1}^{\mathrm{m}} \\ b_1^{\mathrm{m}} \\ b_{-3}^{\mathrm{m}} \end{bmatrix} = \mathbf{Q}_{\mathrm{fm}}\begin{bmatrix} a_3^{\mathrm{f}} \\ b_1^{\mathrm{f}} \end{bmatrix} \tag{21}$$

where the far-field conditions (18) and the equations

$$a_1^{\mathrm{c}} = \mathbf{P}_{\mathrm{mc}}(\mathbf{P}_{\mathrm{fm}}a_1^{\mathrm{f}} + \mathbf{R}_{\mathrm{fm}}) + R_{\mathrm{mc}}, \quad \begin{bmatrix} 0 \\ b_1^{\mathrm{c}} \end{bmatrix} = \mathbf{Q}_{mc}\mathbf{Q}_{fm}\begin{bmatrix} a_3^{\mathrm{f}} \\ b_1^{\mathrm{f}} \end{bmatrix} \tag{22}$$

have been used and Eq. (22) is derived from Eq. (19). The adopted abbreviations are

$$\begin{aligned}
&\mathbf{P}_{\mathrm{fm}} = \begin{bmatrix} 1 + p_{\mathrm{fm}} \\ -2\lambda p_{\mathrm{fm}} \end{bmatrix}, \quad \mathbf{R}_{\mathrm{fm}} = t_{\mathrm{fm}}\begin{bmatrix} 1 \\ -2\lambda \end{bmatrix} \\
&\mathbf{P}_{\mathrm{mc}} = \frac{1}{(1 + p_{\mathrm{cm}} + 2q_{\mathrm{cm}})}[\,(1 + 2q_{\mathrm{cm}}) \quad q_{\mathrm{cm}}\,], \quad R_{\mathrm{mc}} = -\frac{t_{\mathrm{cm}}}{(1 + p_{\mathrm{cm}} + 2q_{\mathrm{cm}})} \\
&\mathbf{Q}_{\mathrm{fm}} = \begin{bmatrix} (1 + p_{\mathrm{fm}} + q_{\mathrm{fm}}) & 0 \\ -3\lambda^2 q_{\mathrm{fm}} & -\lambda q_{\mathrm{fm}} \\ -3\lambda p_{\mathrm{fm}} & 1 + q_{\mathrm{fm}} \\ -\lambda^3(p_{\mathrm{fm}} + 4q_{\mathrm{fm}}) & -\lambda^2 q_{\mathrm{fm}} \end{bmatrix} \\
&\mathbf{Q}_{\mathrm{mc}} = \frac{1}{(1 + p_{\mathrm{cm}} + 2q_{\mathrm{cm}})}\begin{bmatrix} (1 + q_{\mathrm{cm}}) & -q_{\mathrm{cm}} & 0 & q_{\mathrm{cm}} \\ 3p_{\mathrm{cm}} & p_{\mathrm{cm}} + 4q_{\mathrm{cm}} & (1 + p_{\mathrm{cm}} + q_{\mathrm{cm}}) & -3q_{\mathrm{cm}} \end{bmatrix}.
\end{aligned} \tag{23}$$

4. Stress concentrations under thermo-electro-magneto-mechanical coupling loads

Stress concentrations in microstructures play a crucial role in fatigue and fracture of composites. In some cases thermo-electro-magnetic loads may aggravate stress concentrations in piezoelectric–magnetic composites, whereas in other cases they can alleviate such stress concentrations. The present three-phase model can serve as a fiber/interphase/matrix model to study the phenomenon in coated composite materials.

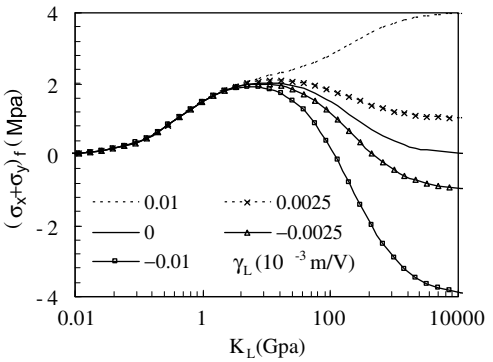

Fig. 2. Variations in the fiber stress with the interphase bulk modulus under a far-field mechanical load coupled with an electrical field for various γ_L.

4.1. Example 1. Two-phase cylinder model for piezoelectric–magnetic fiber composites

This is a special case of the three-phase model. In fact, letting the material properties in the interphase layer and matrix be the same, the present three-phase model degenerates into a two-phase model, and the solution (20) degenerates into

$$\begin{aligned} a_1^f &= \frac{1}{4(1+p_{fm})}(\sigma_1^\infty+\sigma_2^\infty) - \frac{t_{fm}}{(1+p_{fm})} \\ \begin{bmatrix} a_3^f \\ b_1^f \end{bmatrix} &= \begin{bmatrix} 0 \\ 1 \end{bmatrix} \frac{1}{2(1+p_{fm})}(\sigma_2^\infty-\sigma_1^\infty) \end{aligned} \tag{24}$$

From Eqs. (10) and (16), we obtain the stress field in the fiber, and the hydrostatic stress is given by

$$(\sigma_1+\sigma_2)_f = \frac{K_m^{-1}+\mu_m^{-1}}{K_f^{-1}+\mu_m^{-1}}(\sigma_1^\infty+\sigma_2^\infty) + \frac{1}{K_f^{-1}+\mu_m^{-1}}\left[(-\nu_{13f}+\nu_{13m})\varepsilon_3 + \left(\frac{e_{31f}}{2K_f}-\frac{e_{31m}}{2K_m}\right)E_3 + \left(\frac{q_{31f}}{2K_f}-\frac{q_{31m}}{2K_m}\right)H_3 + \left(\frac{\beta_{1f}}{2K_f}-\frac{\beta_{1m}}{2K_m}\right)\theta\right] \tag{25}$$

It is seen that under far-field uniform thermo-electro-magneto-mechanical loads, the stress field in the inclusion (fiber) is uniform, and the stress value is the algebraic sum of those induced by various kinds of loads. When all stresses induced, respectively, by thermal, electric, magnetic and mechanical loads have the same sign, the most serious stress concentration occurs. However, if the magnitude and sign of one or more loads can be adjusted, a zero-stress state can be achieved.

4.2. Example 2. Stress concentration in the inclusion of a three-phase model under thermo-electro-magneto-mechanical coupling loads

The present three-phase fiber/interphase/matrix model can be used to reveal a lot of interesting thermo-electro-magneto-mechanical coupling phenomena in such composites. As an illustrative example, the influence of the piezoelectric interphase layer on fiber stress concentrations is considered.

Suppose that both the fiber and matrix are pure elastic materials with the bulk and shear moduli K_f = 100 GPa, K_m = 1 GPa, G_f = 50 GPa, G_m = 0.5 GPa. The piezoelectric interphase layer has a changeable bulk modulus K_L (while keep $G_L = 0.5K_L$, which means to keep the Poisson's ratio unchanged for an isotropic material). Introduce a new parameter $\gamma = \frac{e_{31}}{2K} = d_{31} + \nu_{13}d_{33}$ to reflect the influence of the piezoelectric material properties. Notice that the definition is analogous to the hydrostatic piezomodulus $d_h = d_{33} + 2d_{31}$, which refer to Shaulov et al. (1989), Grekov et al. (1989), Dunn and Taya (1993). ρ_1:ρ_2 = 1:10,where ρ_1 and ρ_2 are the radii of L_1 and L_2 (Fig. 1), respectively. Apply the far-field loads $\sigma_1^\infty + \sigma_2^\infty = 1$ MPa and E_3 = 1 V/m. The averaged.hydrostatic stress in the fiber is obtained as

$$\langle\sigma_1+\sigma_2\rangle_f = \frac{(1+p_{mL}+2q_{mL})(\sigma_1^\infty+\sigma_2^\infty)}{(1+p_{fL}+2q_{mL})+2(1-\lambda)p_{fL}q_{mL}} - 4\frac{\{[1+2(1-\lambda)q_{mL}](\gamma_f-\gamma_L)-(\gamma_m-\gamma_L)\}}{\{(1+p_{fL}+2q_{mL})+2(1-\lambda)p_{fL}q_{mL}\}}\frac{E_3}{(K_L^{-1}+\mu_L^{-1})} \tag{26}$$

Since both the fiber and matrix are pure elastic materials, we have $\gamma_f = \gamma_m = 0$, the fiber stress versus the interphase bulk modulus curves are plotted in Fig. 2 for various γ_L. It is seen that the very soft or very hard interphase layers both shield the fiber from stresses, whereas a moderate stiffness interphase magnifies the stresses. The maximum stress concentration in the fiber occurs at about $K_L = \sqrt{K_f K_m}$, It is of interest to note that when $K_L < \sqrt{K_f K_m}$, the electrical field E_3 has little influence on the fiber stress concentration, whereas with the increase of K_L, such an influence can rapidly goes up depending on the parameter γ_L.By the way, the influence of the interphase on the stress concentration under antiplane shear coupled with

inplane electrical field has been studied by Jiang and Cheung (2001). Similarly, the coupling effect induced by the magnetic or thermal field can be analyzed. The above discussion shows that the stress control in piezoelectric–magnetic fiber composites can be conducted not only by adjusting the far-field thermo-electro-magneto-mechanical coupling loads, but also by matching the properties of the constituents.

5. Effective thermo-electro-magneto-elastic coupling properties

The present three-phase model can also serve as a fiber/matrix/composite model, whereby the GSCM is developed for piezoelectric–magnetic fiber composites under in-plane mechanical load integrated with thermo-electro-magnetic loads. The GSCM in this paper and that in the reference (Jiang and Cheung, 2001) complement each other, and the latter dealt with the antiplane shear loading coupled with inplane electric field.

5.1. Averaged values of fields

Taking the fiber and matrix ring in the fiber/matrix/composite model as the representative volume element (RVE), we have

$$\langle \bullet \rangle_r = \lambda \langle \bullet \rangle_{\mathrm{f}} + (1-\lambda)\langle \bullet \rangle_{\mathrm{m}} \tag{27}$$

where $\langle \bullet \rangle$ denotes the averaged value of a field and the subscripts r, f and m refer to the RVE, fiber and matrix, respectively.

According to the divergence theorem, the averaged stresses (strains) in the fiber and RVE can be calculated by the surface integration of the stress (displacement) (Nemat-Nasser, 1999), which yields

$$\begin{aligned}
&\langle \sigma_1 + \sigma_2 \rangle_{\mathrm{f}} = 4a_1^{\mathrm{f}} \\
&\langle \varepsilon_1 + \varepsilon_2 \rangle_{\mathrm{f}} = 2K_{\mathrm{f}}^{-1} a_1^{\mathrm{f}} + 2\varepsilon_{\mathrm{f}}^{*} \\
&\langle \sigma_1 + \sigma_2 \rangle_{r} = 4a_1^{\mathrm{m}} + 2b_{-1}^{\mathrm{m}} \\
&\langle \sigma_2 - \sigma_1 \rangle_{r} = 6a_3^{\mathrm{m}} + 2a_{-1}^{\mathrm{m}} + 2b_1^{\mathrm{m}} \\
&\langle \varepsilon_1 + \varepsilon_2 \rangle_{r} = 2K_{\mathrm{m}}^{-1} a_1^{\mathrm{m}} - \mu_{\mathrm{m}}^{-1} b_{-1}^{\mathrm{m}} + 2\varepsilon_{\mathrm{m}}^{*} \\
&\langle \varepsilon_2 - \varepsilon_1 \rangle_{r} = 3\mu_{\mathrm{m}}^{-1} a_3^{\mathrm{m}} - (2K_{\mathrm{m}}^{-1} + \mu_{\mathrm{m}}^{-1}) a_{-1}^{\mathrm{m}} + \mu_{\mathrm{m}}^{-1} b_1^{\mathrm{m}}
\end{aligned} \tag{28}$$

5.2. Effective elastic moduli

The average field theorem is used to predict the effective moduli of a composite. For the GSCM developed in this paper, the generalized average field theorem can lead to three sets of equations with different physical implications.

(a) The average stresses in the RVE are equal to the far-field stresses

$$\langle \sigma_1 + \sigma_2 \rangle_{\mathrm{r}} = (\sigma_1^{\infty} + \sigma_2^{\infty}), \quad \langle \sigma_2 - \sigma_1 \rangle_{\mathrm{r}} = (\sigma_2^{\infty} - \sigma_1^{\infty}) \tag{29}$$

(b) The average strains in the RVE are equal to the far-field strains

$$\langle \varepsilon_1 + \varepsilon_2 \rangle_{\mathrm{r}} = \frac{1}{2} K_{\mathrm{c}}^{-1} (\sigma_1^{\infty} + \sigma_2^{\infty}) + 2\varepsilon_{\mathrm{c}}^{*}, \quad \langle \varepsilon_2 - \varepsilon_1 \rangle_{\mathrm{r}} = \frac{1}{2} \mu_{\mathrm{c}}^{-1} (\sigma_2^{\infty} - \sigma_1^{\infty}) \tag{30}$$

(c) The average stresses and strains in the RVE satisfy the constitutive equations of a composite

$$\langle \varepsilon_1 + \varepsilon_2 \rangle_{\mathrm{r}} = \frac{1}{2} K_{\mathrm{c}}^{-1} \langle \sigma_1 + \sigma_2 \rangle_{\mathrm{r}} + 2\varepsilon_{\mathrm{c}}^{*}, \quad \langle \varepsilon_2 - \varepsilon_1 \rangle_{\mathrm{r}} = \frac{1}{2} \mu_{\mathrm{c}}^{-1} \langle \sigma_2 - \sigma_1 \rangle_{\mathrm{r}} \tag{31}$$

It is seen that the three sets of equations i.e. Eqs. (29)–(31) are equivalent, and a proof is given in the Appendix A. This proof shows that the fiber and matrix ring in the three-phase model constitute a RVE, and it provides also a strong evidence of mathematical rigor in their elasticity formulation and physical realism of the GSCM.

Solving any one of the three sets of Eqs. (29)–(31), we obtain the normalized parameters p_{cm} and t_{cm} for the inplane bulk modulus and eigenstrain (refer to Eq. (14))

$$p_{\mathrm{cm}} = \frac{\lambda p_{\mathrm{fm}}}{1 + (1-\lambda) p_{\mathrm{fm}}}, \quad t_{\mathrm{cm}} = \frac{\lambda t_{\mathrm{fm}}}{1 + (1-\lambda) p_{\mathrm{fm}}} \tag{32}$$

The normalized parameter for the shear modulus q_{cm} is determined by the following equation

$$
\begin{aligned}
&Aq_{cm}^2 + Bq_{cm} + C = 0\\
&A = -(1 + p_{fm} + q_{fm})[1 + (1-\lambda)^4 q_{fm}] + \lambda^3 p_{fm} + \lambda^4 q_{fm}\\
&B = -(1 + p_{fm} + q_{fm})[1 + q_{fm}(1 - 2\lambda + \lambda^4)] + \lambda^4 q_{fm}\\
&C = (1 + p_{fm} + q_{fm})\lambda q_{fm}.
\end{aligned}
\tag{33}
$$

5.3. Effective thermo-electro-magneto-elastic coupling moduli

Recast the constitutive Eq. (9) as

$$
\begin{aligned}
&\begin{bmatrix} (\sigma_1 + \sigma_2) \\ \sigma_3 \\ D_3 \\ B_3 \end{bmatrix} = \mathbf{M} \begin{bmatrix} \varepsilon_3 \\ E_3 \\ H_3 \\ \theta \end{bmatrix} + \mathbf{N}(\varepsilon_1 + \varepsilon_2)\\
&\mathbf{M} = \begin{bmatrix} 4v_{13}K & -2e_{31} & -2q_{31} & -2\beta_1 \\ (4Kv_{13}^2 + E_3) & -e_{33} & -q_{33} & -\beta_3 \\ e_{33} & k_{33} & \alpha_{33} & p_3 \\ q_{33} & \alpha_{33} & \mu_{33} & m_3 \end{bmatrix}, \quad \mathbf{N} = \begin{bmatrix} 2K \\ 2v_{13}K \\ e_{31} \\ q_{31} \end{bmatrix}
\end{aligned}
\tag{34}
$$

By using the theorem of averaged field, and noting Eq. (28), the coupled modulus in the matrix **M** can be obtained as

$$
\mathbf{M}_c = \lambda \mathbf{M}_f + (1-\lambda)\mathbf{M}_m + \lambda \eta_K (\mathbf{N}_f - \mathbf{N}_m)\left[\mathbf{M}_{1m} + \lambda \frac{K_f}{K_m}(\mathbf{M}_{1f} - \mathbf{M}_{1m})\right] \tag{35}
$$

where $\mathbf{M}_{1f}$, $\mathbf{M}_{1m}$ are row vectors, which are composed of the first rows of the matrices $\mathbf{M}_f$, $\mathbf{M}_m$, respectively

$$
\begin{aligned}
&\mathbf{M}_{1f} = [\,4v_{13f}K_f \quad -2e_{31f} \quad -2q_{31f} \quad -2\beta_{1f}\,],\\
&\mathbf{M}_{1m} = [\,4v_{13m}K_m \quad -2e_{31m} \quad -2q_{31m} \quad -2\beta_{1m}\,]
\end{aligned}
\tag{36}
$$

and

$$
\eta_K = \frac{K_m + \mu_m}{\mu_m + \lambda K_m + (1-\lambda)K_f} \tag{37}
$$

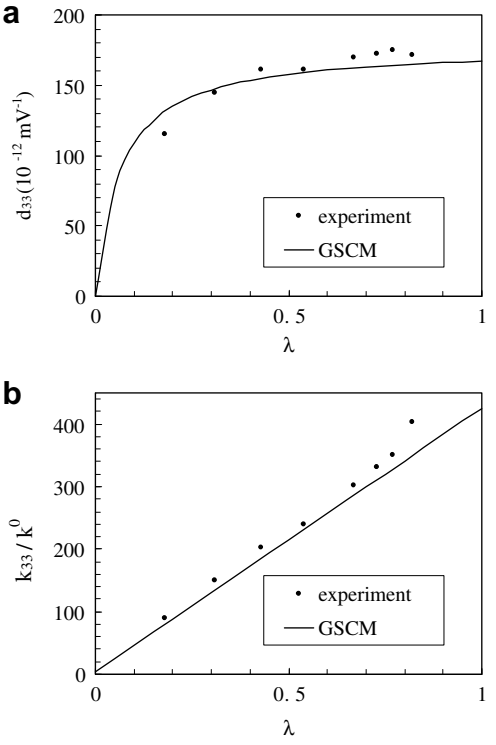

Fig. 3. A comparison of the present GSCM predictions with experimental data (Chan and Unsworth, 1989) for PZT-7A/Araldite D. (a) Effective d_{33} versus λ; (b) effective k_{33}/k^0 versus λ.

Now all the effective thermo-electro-magneto-elastic moduli have been obtained in compact explicit form, and their detailed expressions are listed in Appendix B for reference.

5.4. Comparison of the GSCM predictions with experimental results

It is of interest to compare the present GSCM predictions with existing experimental data. The effective piezoelectric strain modulus d_{33} and dielectric permeability k_{33} versus the fiber volume fraction λ diagrams are plotted in Fig. 3a and b, respectively. For a piezoelectric ceramic/polymer 1–3 composite used in an ultrasonic transducer, the experiment data are quoted from Chan and Unsworth (1989), and the material constants are

$$\begin{aligned} &C_{11} = 148\ \text{GPa}, \quad C_{12} = 76.2\ \text{GPa}, \quad C_{13} = 74.2\ \text{GPa}, \quad C_{33} = 131\ \text{GPa} \\ \text{PZT-7A}: &d_{31} = -60 \times 10^{-12}\ \text{mV}^{-1}, \quad d_{33} = 167 \times 10^{-12}\ \text{mV}^{-1}, \quad k_{33}/k^0 = 425 \\ &(k^0 = 8.85 \times 10^{-12}\text{C}^2\text{N}^{-1}\text{m}^{-2}) \\ \text{Araldite D}: &C_{11} = C_{33} = 8\ \text{GPa}, \quad C_{12} = C_{13} = 4.4\ \text{GPa}, \quad d_{31} = d_{33} = 0, \quad k_{33}/k_0 = 4 \end{aligned}$$

Chan and Unsworth pointed out that the PZT-7A ceramic samples have different moduli according to manufacturer's data. In their experiment, the measured piezoelectric strain modulus is $d_{33} = 167 \times 10^{-12}$ m/V instead of $d_{33} = 150 \times 10^{-12}$ m/V used in the engineering handbook. It is seen that the present GSCM predictions are in good agreement with the experiment results. At a high volume fraction, the GSCM seems to give slightly lower estimates, which may be worthy of studied further.

5.5. Enhancement of d_{31} and ρ_1

It is well known that composite materials can provide much superior properties than any of their monolithic constituent materials, and the effective moduli of some composites may significantly exceeds those of the constituent phases. Such a marvelous enhancement phenomenon was discussed on the effective d_{31} by Smith et al. (1985), Shaulov et al. (1989) and on effective ρ_1 by Dunn (1993), Levin et al. (1999). The present GSCM is useful in understanding such thermo-electro-magneto-elastic coupling behavior. As an illustrative example, consider the two composites (Pb,Ca)TiO_3/stycast; $BaTiO_3$/polymer with the following material constants

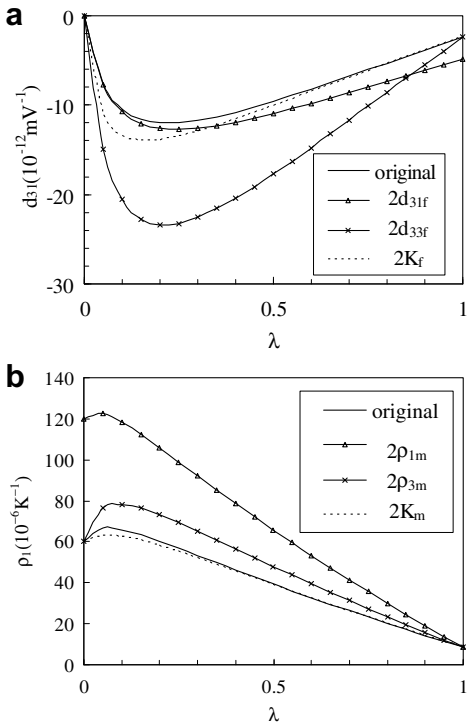

Fig. 4. Enhancement of effective moduli (original composite: (Pb,Ca)TiO_3/Stycast; $BaTiO_3$/polymer; $2d_{31f}$: value of d_{31} for fiber is twice the original; $2d_{33f}$: value of d_{33} for fiber is twice the original; $2K_f$: value of K for fiber is twice the original; $2\rho_{1m}$: value of ρ_1 for matrix is twice the original; $2\rho_{3m}$: value of ρ_3 for matrix is twice the original; $2K_m$: value of K for matrix is twice the original). (a) Effective d_{31} versus λ for (Pb,Ca)TiO_3/stycast composite; (b) effective ρ_1 versus λ for $BaTiO_3$/polymer composite.

$$(Pb,Ca)TiO_3: C_{11} = 149\ \text{GPa},\quad C_{12} = 34.5\ \text{GPa},\quad C_{13} = 30.3\ \text{GPa},\quad C_{33} = 128\ \text{GPa}$$
$$d_{31} = -2.4\times10^{-12}\ \text{mV}^{-1},\quad d_{33} = 70\times10^{-12}\ \text{mV}^{-1},\quad k_{33}/k^0 = 207$$
$$\text{Stycast polymer}: C_{11} = C_{33} = 12.3\ \text{GPa},\quad C_{12} = C_{13} = 5.2\ \text{GPa},\quad d_{31} = d_{33} = 0,\quad k_{33}/k_0 = 4$$
$$BaTiO_3: C_{11} = 150\ \text{GPa},\quad C_{12} = C_{13} = 66\ \text{GPa},\quad C_{33} = 146\ \text{GPa}$$
$$\rho_1 = 8.53\times10^{-6}\ \text{K}^{-1},\quad \rho_{33} = 1.99\times10^{-6}\ \text{K}^{-1}$$
$$\text{Polymer}: C_{11} = C_{33} = 8\ \text{GPa},\quad C_{12} = C_{13} = 4.4\ \text{GPa},\quad \rho_1 = \rho_{33} = 60\times10_{-6}\ \text{K}_{-1}$$

The curves of the effective moduli d_{31} and ρ_1 versus λ are plotted in Fig. 4a and b, where each component of the moduli for the fiber and matrix is taken twice in turn to examine their respective influences. From Fig. 4, marvelous enhancement effect for the effective moduli can be observed. It is also found that such an enhancement effect not only depends on the corresponding moduli of the constituents, but also on other moduli of the constituents with various sensitivities. It is noted that an analogous enhancement has also been found for elastic moduli of a piezocomposite (Levin et al., 1999; Jiang et al., 2001).

5.6. Parallel and product properties in piezoelectric–magnetic fiber composites

piezoelectric–magnetic fiber composites exhibit a new material property – the magnetoelectric (ME) coupling effect, which is absent in the individual phases and is known as the product property (Ryu et al., 2002). The present GSCM can be used to predict such a peculiar product property. From Eq. (35), the explicit expression of the ME coefficient α_{33c} can be written as

$$\alpha_{33c} = \lambda\alpha_{33f} + (1-\lambda)\alpha_{33m} + \lambda(1-\lambda)\frac{(e_{31f}-e_{31m})(q_{31f}-q_{31m})}{\mu_m + \lambda K_m + (1-\lambda)K_f} \tag{38}$$

The formula is also presented by Benveniste (1995), in which, his formula is derived from the composite cylinder model by using the exact connections. It is seen that the above formula are composed of two parts: the first two terms are due to the parallel effect of the ME coefficient, and the third term reflects the product properties of the piezoelectric and piezomagnetic constituents.

Consider the optimization of the ME coefficient α_{33} in a piezoelectric/piezomagnetic composite. Take the derivative of Eq. (38) with respect to the fiber volume fraction λ, we have

$$\lambda = \frac{\sqrt{\mu_m + K_f}}{\sqrt{\mu_m + K_f} + \sqrt{\mu_m + K_m}} \rightarrow (\alpha_{33c})_{max} = \frac{(e_{31f}-e_{31m})(q_{31f}-q_{31m})}{\left(\sqrt{\mu_m + K_f} + \sqrt{\mu_m + K_m}\right)^2} \tag{39}$$

Take the $BaTiO_3/CoFe_2O_4$ composite as an example, where the material constants are

$$BaTiO_3: C_{11} = 166.2\ \text{GPa},\quad C_{12} = 76.5\ \text{GPa},\quad C_{13} = 77.4\ \text{GPa},\quad C_{33} = 161.4\ \text{GPa}$$
$$e_{31} = -4.22\text{C m}^{-2},\quad e_{33} = 18.6\ \text{C m}^{-2},\quad k_{33}/k^0 = 1350,\quad \mu_{33} = 10\times10^{-6}\text{N S}^2\ \text{C}^{-2}$$
$$CoFe_2O_4: C_{11} = 286\ \text{GPa},\quad C_{12} = 173\ \text{GPa},\quad C_{13} = 170.5\ \text{GPa},\quad C_{33} = 269.5\ \text{GPa}$$
$$q_{31} = 580.3\text{NA}^{-1}\text{m}^{-1},\quad q_{33} = 699.7\text{NA}^{-1}\text{m}^{-1},\quad k_{33}/k^0 = 10,\quad \mu_{33} = 157\times10^{-6}\text{NS}^2\text{C}^{-2}$$

The ME coefficient α_{33} versus the volume fraction λ of $BaTiO_3$ curves are plotted in Fig. 5. It is seen that when $BaTiO_3$ is used as the fiber material and $CoFe_2O_4$ is used as the matrix material, the ME coefficient α_{33c} arrives at a maximum 2.68 at $\lambda = 0.44$; whereas when $CoFe_2O_4$ is used as the fiber material and $BaTiO_3$ is used as the matrix material, the ME coefficient α_{33c} arrives at a maximum 2.82 at the same $\lambda = 0.44$ (in the former λ means the volume fraction of the fiber $BaTiO_3$, whereas in the latter it means the volume fraction of the matrix $BaTiO_3$). The two curves seem to show that a soft matrix causes a higher value of α_{33c}. To verify this, introduce a dimensionless modulus coefficient η, and consider four cases:

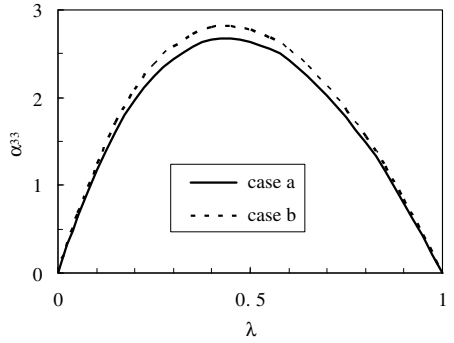

Fig. 5. Optimization of ME coefficient with fiber volume fraction. Case a: $BaTiO_3$ is used as the fiber material Case a: $BaTiO_3$ is used as the matrix material.

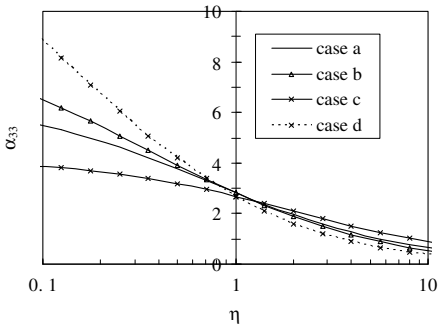

Fig. 6. Optimization of ME coefficient with the phase elastic moduli. Case a: change the modulus of the fiber CoFe2O4 and let $\eta = K_f/K^0$, case b: change the modulus of the matrix BaTiO3 and let $\eta = K_m/K^0$, case c: change the modulus of the fiber BaTiO3 and let $\eta = K_f/K^0$, case d: change the modulus of the matrix CoFe2O4 and let $\eta = K_m/K^0$.

Case a: change the modulus of the fiber $CoFe_2O_4$ and let $\eta = K_f/K^0$
Case b: change the modulus of the matrix $BaTiO_3$ and let $\eta = K_m/K^0$
Case c: change the modulus of the fiber $BaTiO_3$ and let $\eta = K_f/K^0$
Case d: change the modulus of the matrix $CoFe_2O_4$ and let $\eta = K_m/K^0$

The maximum value of α_{33c} versus η curves for the four cases are plotted in Fig. 6, where other material constants remain unchanged. This figure shows that to obtain a high value of α_{33c}, one should choose soft matrix and hard fiber. An efficient way to obtain a large ME coefficient is to reduce the stiffness modulus of the matrix, especially when it is harder than the fiber.

Inspired by the above product property of piezoelectric–magnetic fiber composites, some researchers thought that ME effect could also be obtained by thermal interaction in a pyroelectric–pyromagnetic composite, but so far no theoretical or experimental results were reported. According to Eq. (38), the ME effect is independent of the pyroelectric or pyromagnetic properties. Although the thermal expansion of a material induces thermal strain and in turn induces thermal stress which can be transformed into electric or magnetic effect as well as the strain itself, however, thermal load cannot be induced in a reversed manner hence such a guess could not be correct.

6. Conclusion

A three-phase model for analyzing thermo-electro-magneto-elastic coupling properties is presented for piezoelectric–magnetic fiber composites. To overcome the mathematical difficulties in solving the complex multi-field coupling problem, an eigenstrain corresponding to the thermo-electro-magneto-elastic effect is introduced, whereby the problem is reduced to a formal in-plane elasticity problem and exact closed form solutions are available.

The present three-phase model can be applied to fiber/interphase/matrix composites. Numerical examples are presented to show stress concentrations under thermo-electro-magneto-mechanical coupling loads. It is seen that in some cases thermo-electro-magnetic loads may aggravate stress concentrations in piezoelectric–magnetic composites, whereas in other cases they can alleviate such stress concentrations, which is useful in fatigue and fracture analysis and strength design of piezoelectric–magnetic fiber composites.

The present model can also be applied to fiber/matrix composites, whereby a generalized self-consistent method (GSCM) is developed for predicting the effective properties of piezoelectric–magnetic fiber reinforced composites. The predictions for the effective piezoelectric, piezomagnetic, thermoelectric and magnetoelectric moduli are given in compact explicit form, which are in good agreement with available experiment data. It is noted that the present method can well model the marvelous enhancement effect and peculiar product properties of effective moduli in piezoelectric–magnetic fiber composites. As a theoretical basis for the GSCM, the three different sets of equations in predicting the effective properties are proved to be equivalent.

Acknowledgements

The work is supported by the National Natural Science Foundation of China under Grant NNSFC 10672008 and the Hong Kong Research Grants council under Project HKU7011/01E.

Appendix A. Proof of the equivalence of Eqs. (29)–(31)

In Section 5, it is pointed out that the three sets of equations i.e. Eqs. (29)–(31) are equivalent. In the following the proposition will be proved for the inplane bulk and shear moduli, respectively.

A.1. For the inplane bulk modulus

First consider Eq. (29). The substitution of Eq. (20) into Eq. (28) and then into Eq. (29) yields

$$\begin{aligned}\langle\sigma_1+\sigma_2\rangle_r &= [\,4 \quad 2\,]\begin{bmatrix} a_1^{\mathrm{m}} \\ b_{-1}^{\mathrm{m}}\end{bmatrix} = [\,4 \quad 2\,](P_{\mathrm{fm}}a_1^{\mathrm{f}}+R_{\mathrm{fm}}) \\ &= [\,4 \quad 2\,]\begin{bmatrix} 1+p_{\mathrm{fm}} \\ -2fp_{\mathrm{fm}}\end{bmatrix}\frac{(1+p_{\mathrm{cm}}+2q_{\mathrm{cm}})\frac{1}{4}(\sigma_1^{\infty}+\sigma_2^{\infty})-[1+2(1-\lambda)q_{\mathrm{cm}}]t_{\mathrm{fm}}+t_{\mathrm{cm}}}{(1+p_{\mathrm{fm}}+2q_{\mathrm{cm}})+2(1-\lambda)p_{\mathrm{fm}}q_{\mathrm{cm}}}+t_{\mathrm{fm}}4(1-\lambda) \\ &= [4+4(1-\lambda)p_{\mathrm{fm}}]\frac{(1+p_{\mathrm{cm}}+2q_{\mathrm{cm}})\frac{1}{4}(\sigma_1^{\infty}+\sigma_2^{\infty})-[1+2(1-\lambda)q_{\mathrm{cm}}]t_{\mathrm{fm}}+t_{\mathrm{cm}}}{(1+p_{\mathrm{fm}}+2q_{\mathrm{cm}})+2(1-\lambda)p_{\mathrm{fm}}q_{\mathrm{cm}}}+t_{\mathrm{fm}}4(1-\lambda) \\ &= (\sigma_1^{\infty}+\sigma_2^{\infty})\end{aligned} \tag{A1}$$

Regarding $(\sigma_1^{\infty}+\sigma_2^{\infty})$ as a variable and let its zeroth- and first-order coefficients on both sides of Eq. (A1) be equal, we have

$$\begin{aligned}&[1+(1-\lambda)p_{\mathrm{fm}}](1+p_{\mathrm{cm}}+2q_{\mathrm{cm}}) = (1+p_{\mathrm{fm}}+2q_{\mathrm{cm}})+2(1-\lambda)p_{\mathrm{fm}}q_{\mathrm{cm}} \\ &[1+2(1-\lambda)q_{\mathrm{cm}}]t_{\mathrm{fm}}-t_{\mathrm{cm}} = (1+p_{\mathrm{cm}}+2q_{\mathrm{cm}})t_{\mathrm{fm}}(1-\lambda)\end{aligned} \tag{A2}$$

The simplification of Eqs. (A2) leads to Eq. (32).

Then consider Eq. (29). The substitution of Eq. (20) into Eq. (28) and then into Eq. (30) yields

$$[\,2K_{\mathrm{m}}^{-1} \quad -\mu_{\mathrm{m}}^{-1}\,]\begin{bmatrix} a_1^{\mathrm{m}} \\ b_{-1}^{\mathrm{m}}\end{bmatrix} = \frac{1}{2}K_{\mathrm{c}}^{-1}[\,4 \quad 2\,]\begin{bmatrix} a_1^{\mathrm{m}} \\ b_{-1}^{\mathrm{m}}\end{bmatrix} + 2\varepsilon_{\mathrm{c}}^{*} - 2\varepsilon_{\mathrm{m}}^{*} \tag{A3}$$

Dividing both sides of Eq. (A3) by $(K_{\mathrm{m}}^{-1}+\mu_{\mathrm{m}}^{-1})$, we have

$$\begin{aligned}-2t_{\mathrm{cm}} &= [2p_{\mathrm{cm}}1+p_{\mathrm{cm}}](P_{\mathrm{fm}}a_1^{\mathrm{f}}+R_{\mathrm{fm}}) \\ &= [2(1+p_{\mathrm{fm}})p_{\mathrm{cm}}-2\lambda p_{\mathrm{fm}}(1+p_{\mathrm{cm}})]\frac{(1+p_{\mathrm{cm}}+2q_{\mathrm{cm}})a_1^{\mathrm{c}}-[1+2(1-\lambda)q_{\mathrm{cm}}]t_{\mathrm{fm}}+t_{\mathrm{cm}}}{(1+p_{\mathrm{fm}}+2q_{\mathrm{cm}})+2(1-\lambda)p_{\mathrm{fm}}q_{\mathrm{cm}}} \\ &\quad +[2p_{\mathrm{cm}}-2\lambda(1+p_{\mathrm{cm}})]t_{\mathrm{fm}}\end{aligned} \tag{A4}$$

Regarding $(\sigma_1^{\infty}+\sigma_2^{\infty})$ as a variable and let its zeroth- and first-order coefficients on both sides of Eq. (A4) be equal, we have

$$\begin{aligned}0 &= (1+p_{\mathrm{fm}})p_{\mathrm{cm}}-\lambda p_{\mathrm{fm}}(1+p_{\mathrm{cm}}) \\ -t_{\mathrm{cm}} &= [-\lambda+(1-\lambda)p_{\mathrm{cm}}]t_{\mathrm{fm}}\end{aligned} \tag{A5}$$

The equation also leads to Eq. (32).

Obviously, Eq. (31) can be derived by using Eqs. (29) and (30). The proposition is proved for the bulk modulus, where p_{cm} can be egarded as a normalized bulk modulus.

A.2. For the inplane shear modulus

Using Eqs. (28) and (29), we have

$$(\sigma_2^{\infty}-\sigma_1^{\infty}) = \langle\sigma_2-\sigma_1\rangle_{\mathrm{r}} = [\,6 \quad 2 \quad 2 \quad 0\,]\big[\,a_3^{\mathrm{m}} \quad a_{-1}^{\mathrm{m}} \quad b_1^{\mathrm{m}} \quad b_{-3}^{\mathrm{m}}\,\big]^{\mathrm{T}} \tag{A6}$$

The substitution of Eq. (23) into the far-field conditions yields

$$Q_{\mathrm{mc}}\big[\,a_3^{\mathrm{m}} \quad a_{-1}^{\mathrm{m}} \quad b_1^{\mathrm{m}} \quad b_{-3}^{\mathrm{m}}\,\big]^{\mathrm{T}} - \begin{bmatrix}0\\1\end{bmatrix}\frac{1}{2}(\sigma_2^{\infty}-\sigma_1^{\infty}) = 0 \tag{A7}$$

and

$$\begin{bmatrix}(1+q_{\mathrm{cm}}) & -q_{\mathrm{cm}} & 0 & q_{\mathrm{cm}} \\ -3-6q_{\mathrm{cm}} & 2q_{\mathrm{cm}}-1 & -q_{\mathrm{cm}} & -3q_{\mathrm{cm}}\end{bmatrix}Q_{\mathrm{fm}}\begin{bmatrix}a_3^{\mathrm{f}}\\ b_1^{\mathrm{f}}\end{bmatrix} = \begin{bmatrix}0\\0\end{bmatrix} \tag{A8}$$

The above equations have non-zero solutions for $a_3^{\mathrm{f}}, b_1^{\mathrm{f}}$ and the matrix order decreases. From Eq. (A7), we have

$$\begin{aligned}&a_{11}a_{22}-a_{12}a_{21} = 0 \\ &a_{11} = (1+p_{\mathrm{fm}}+q_{\mathrm{fm}})(1+q_{\mathrm{cm}})+3\lambda^2q_{\mathrm{fm}}q_{\mathrm{cm}}-\lambda^3(p_{\mathrm{fm}}+4q_{\mathrm{fm}})q_{\mathrm{cm}} \\ &a_{12} = \lambda q_{\mathrm{fm}}q_{\mathrm{cm}}-\lambda^2q_{\mathrm{fm}}q_{\mathrm{cm}} \\ &a_{21} = (1+p_{\mathrm{fm}}+q_{\mathrm{fm}})(-3-6q_{\mathrm{cm}})-3\lambda^2q_{\mathrm{fm}}(2q_{\mathrm{cm}}-1)+3\lambda p_{\mathrm{fm}}q_{\mathrm{cm}}+\lambda^3(p_{\mathrm{fm}}+4q_{\mathrm{fm}})3q_{\mathrm{cm}} \\ &a_{22} = -\lambda q_{\mathrm{fm}}(2q_{\mathrm{cm}}-1)-(1+q_{\mathrm{fm}})q_{\mathrm{cm}}+\lambda^2q_{\mathrm{fm}}3q_{\mathrm{cm}}\end{aligned} \tag{A9}$$

Simplification of Eq. (A8) leads to Eq. (33).

Similarly, rewrite the average strain and stress as

$$\begin{aligned}\langle \varepsilon_2 - \varepsilon_1 \rangle_r &= \begin{bmatrix} 3\mu_{\mathrm{m}}^{-1} & -(2K_{\mathrm{m}}^{-1} + \mu_{\mathrm{m}}^{-1}) & \mu_{\mathrm{m}}^{-1} & 0 \end{bmatrix} \begin{bmatrix} a_3^{\mathrm{m}} & a_{-1}^{\mathrm{m}} & b_1^{\mathrm{m}} & b_{-3}^{\mathrm{m}} \end{bmatrix}^{\mathrm{T}} \\ \langle \sigma_2 - \sigma_1 \rangle_r &= \begin{bmatrix} 6 & 2 & 2 & 0 \end{bmatrix} \begin{bmatrix} a_3^{\mathrm{m}} & a_{-1}^{\mathrm{m}} & b_1^{\mathrm{m}} & b_{-3}^{\mathrm{m}} \end{bmatrix}^{\mathrm{T}} \end{aligned} \tag{A10}$$

Substituting them into Eq. (31), we have

$$\frac{1}{4(K_{\mathrm{m}}^{-1} + \mu_{\mathrm{m}}^{-1})} [\mu_{\mathrm{c}}^{-1} \langle \sigma_2 - \sigma_1 \rangle_r - \langle \varepsilon_2 - \varepsilon_1 \rangle_r] = \begin{bmatrix} 3q_{\mathrm{cm}} & 1 + q_{\mathrm{cm}} & q_{\mathrm{cm}} & 0 \end{bmatrix} Q_{\mathrm{fm}} \begin{bmatrix} a_3^{\mathrm{f}} \\ b_1^{\mathrm{f}} \end{bmatrix} = 0 \tag{A11}$$

As the first equation of Eq. (A7) is derived by the far-field conditions, it is always satisfied. The second equation of Eqs. (A7) and (A10) are results of Eqs. (29) and (31), respectively. Apparently, the two equations can also be derived by using the first equation of Eq. (A7). The proposition for the shear modulus is thus proved.

Appendix B. The detailed expressions of the effective thermo-electro-magneto-elastic coupled moduli

For the convenience of engineering analysis, the detailed expressions of the effective thermo-electro-magneto-elastic moduli derived in Section 5 are listed as follows:

$$K_{\mathrm{c}} = \lambda K_{\mathrm{f}} + (1-\lambda) K_{\mathrm{m}} - \lambda(1-\lambda) \frac{(K_{\mathrm{f}} - K_{\mathrm{m}})^2}{\mu_{\mathrm{m}} + \lambda K_{\mathrm{m}} + (1-\lambda) K_{\mathrm{f}}} \tag{B1}$$

$$v_{13\mathrm{c}} = \lambda v_{13\mathrm{f}} + (1-\lambda) v_{13\mathrm{m}} + \lambda(1-\lambda) \frac{(K_{\mathrm{f}} - K_{\mathrm{m}})(v_{13\mathrm{f}} - v_{13\mathrm{m}})}{(1-\lambda) K_{\mathrm{m}} \mu_{\mathrm{m}} + (K_{\mathrm{m}} + \lambda \mu_{\mathrm{m}}) K_{\mathrm{f}}} \tag{B2}$$

$$E_{3\mathrm{c}} = \lambda E_{3\mathrm{f}} + (1-\lambda) E_{3\mathrm{m}} + 4\lambda(1-\lambda) \frac{\mu_{\mathrm{m}} K_{\mathrm{m}} K_{\mathrm{f}} (v_{13\mathrm{f}} - v_{13\mathrm{m}})^2}{(1-\lambda) K_{\mathrm{m}} \mu_{\mathrm{m}} + (K_{\mathrm{m}} + \lambda \mu_{\mathrm{m}}) K_{\mathrm{f}}} \tag{B3}$$

$$e_{31\mathrm{c}} = \lambda e_{31\mathrm{f}} + (1-\lambda) e_{31\mathrm{m}} - \lambda(1-\lambda) \frac{(K_{\mathrm{f}} - K_{\mathrm{m}})(e_{31\mathrm{f}} - e_{31\mathrm{m}})}{\mu_{\mathrm{m}} + \lambda K_{\mathrm{m}} + (1-\lambda) K_{\mathrm{f}}} \tag{B4}$$

$$e_{33\mathrm{c}} = \lambda e_{33\mathrm{f}} + (1-\lambda) e_{33\mathrm{m}} - 2\lambda(1-\lambda) \frac{(K_{\mathrm{f}} v_{13\mathrm{f}} - K_{\mathrm{m}} v_{13\mathrm{m}})(e_{31\mathrm{f}} - e_{31\mathrm{m}})}{\mu_{\mathrm{m}} + \lambda K_{\mathrm{m}} + (1-\lambda) K_{\mathrm{f}}} \tag{B5}$$

$$\alpha_{33\mathrm{c}} = \lambda \alpha_{33\mathrm{f}} + (1-\lambda) \alpha_{33\mathrm{m}} + \lambda(1-\lambda) \frac{(e_{31\mathrm{f}} - e_{31\mathrm{m}})(q_{31f} - q_{31\mathrm{m}})}{\mu_{\mathrm{m}} + \lambda K_{\mathrm{m}} + (1-\lambda) K_{\mathrm{f}}} \tag{B6}$$

$$k_{33\mathrm{c}} = \lambda k_{33\mathrm{f}} + (1-\lambda) k_{33\mathrm{m}} + \lambda(1-\lambda) \frac{(e_{31\mathrm{f}} - e_{31\mathrm{m}})^2}{\mu_{\mathrm{m}} + \lambda K_{\mathrm{m}} + (1-\lambda) K_{\mathrm{f}}} \tag{B7}$$

$$q_{31\mathrm{c}} = \lambda q_{31\mathrm{f}} + (1-\lambda) q_{31\mathrm{m}} - \lambda(1-\lambda) \frac{(K_{\mathrm{f}} - K_{\mathrm{m}})(q_{31\mathrm{f}} - q_{31\mathrm{m}})}{\mu_{\mathrm{m}} + \lambda K_{\mathrm{m}} + (1-\lambda) K_{\mathrm{f}}} \tag{B8}$$

$$q_{33\mathrm{c}} = \lambda q_{33\mathrm{f}} + (1-\lambda) q_{33\mathrm{m}} - 2\lambda(1-\lambda) \frac{(K_{\mathrm{f}} v_{13\mathrm{f}} - K_{\mathrm{m}} v_{13\mathrm{m}})(q_{31\mathrm{f}} - q_{31\mathrm{m}})}{\mu_{\mathrm{m}} + \lambda K_{\mathrm{m}} + (1-\lambda) K_{\mathrm{f}}} \tag{B9}$$

$$\mu_{33\mathrm{c}} = \lambda \mu_{33\mathrm{f}} + (1-\lambda) \mu_{33\mathrm{m}} + \lambda(1-\lambda) \frac{(q_{31\mathrm{f}} - q_{31\mathrm{m}})^2}{\mu_{\mathrm{m}} + \lambda K_{\mathrm{m}} + (1-\lambda) K_{\mathrm{f}}} \tag{B10}$$

$$\beta_{1\mathrm{c}} = \lambda \beta_{1\mathrm{f}} + (1-\lambda) \beta_{1\mathrm{m}} - \lambda(1-\lambda) \frac{(K_{\mathrm{f}} - K_{\mathrm{m}})(\beta_{1\mathrm{f}} - \beta_{1\mathrm{m}})}{\mu_{\mathrm{m}} + \lambda K_{\mathrm{m}} + (1-\lambda) K_{\mathrm{f}}} \tag{B11}$$

$$\beta_{3\mathrm{c}} = \lambda \beta_{3\mathrm{f}} + (1-\lambda) \beta_{3\mathrm{m}} - 2\lambda(1-\lambda) \frac{(K_{\mathrm{f}} v_{13f} - K_{\mathrm{m}} v_{13\mathrm{m}})(\beta_{1\mathrm{f}} - \beta_{1\mathrm{m}})}{\mu_{\mathrm{m}} + \lambda K_{\mathrm{m}} + (1-\lambda) K_{\mathrm{f}}} \tag{B12}$$

$$p_{3\mathrm{c}} = \lambda p_{3\mathrm{f}} + (1-\lambda) p_{3\mathrm{m}} + \lambda(1-\lambda) \frac{(e_{31\mathrm{f}} - e_{31\mathrm{m}})(\beta_{1\mathrm{f}} - \beta_{1\mathrm{m}})}{\mu_{\mathrm{m}} + \lambda K_{\mathrm{m}} + (1-\lambda) K_{\mathrm{f}}} \tag{B13}$$

$$m_{3\mathrm{c}} = \lambda m_{3\mathrm{f}} + (1-\lambda) m_{3\mathrm{m}} + \lambda(1-\lambda) \frac{(q_{31\mathrm{f}} - q_{31\mathrm{m}})(\beta_{1\mathrm{f}} - \beta_{1\mathrm{m}})}{\mu_{\mathrm{m}} + \lambda K_{\mathrm{m}} + (1-\lambda) K_{\mathrm{f}}} \tag{B14}$$

The other moduli such as $d_{31\mathrm{c}}$, $d_{33\mathrm{c}}$, $g_{31\mathrm{c}}$, $g_{33\mathrm{c}}$, $\rho_{1\mathrm{c}}$, $\rho_{3\mathrm{c}}$ can be calculated by using the relationship of Eq. (6) or (7), for example, the thermal expansion coefficients $\rho_{1\mathrm{c}}$, $\rho_{3\mathrm{c}}$ are given by the following equations

$$E_{3\mathrm{c}} \rho_{3\mathrm{c}} = \lambda E_{3\mathrm{f}} \rho_{3\mathrm{f}} + (1-\lambda) E_{3\mathrm{m}} \rho_{3\mathrm{m}} + 4\lambda(1-\lambda) \frac{\mu_{\mathrm{m}} K_{\mathrm{m}} (v_{13\mathrm{f}} - v_{13\mathrm{m}})(\rho_{1\mathrm{f}} + v_{13\mathrm{f}} \rho_{3\mathrm{f}} - \rho_{1\mathrm{m}} - v_{13\mathrm{m}} \rho_{3\mathrm{m}})}{(1-\lambda) K_{\mathrm{m}} \mu_{\mathrm{m}} + (K_{\mathrm{m}} + \lambda \mu_{\mathrm{m}}) K_{\mathrm{f}}} \tag{B15}$$

$$\rho_{1\mathrm{c}} + v_{13\mathrm{c}} \rho_{3\mathrm{c}} = \lambda(\rho_{1\mathrm{f}} + v_{13\mathrm{f}} \rho_{3\mathrm{f}}) + (1-\lambda)(\rho_{1m} + v_{13\mathrm{m}} \rho_{3\mathrm{m}}) + \lambda(1-\lambda) \frac{\mu_{\mathrm{m}} (K_{\mathrm{f}} - K_{\mathrm{m}})(\rho_{1\mathrm{f}} + v_{13\mathrm{f}} \rho_{3\mathrm{f}} - \rho_{1\mathrm{m}} - v_{13\mathrm{m}} \rho_{3\mathrm{m}})}{(1-\lambda) K_{\mathrm{m}} \mu_{\mathrm{m}} + (K_{\mathrm{m}} + \lambda \mu_{\mathrm{m}}) K_{\mathrm{f}}}. \tag{B16}$$

References

Benveniste, Y., 1987. A new approach to the application of Mori–Tanaka's theory in composite materials. Mechanics of Materials 6, 147–157.

Benveniste, Y., 1995. Magnetoelectric effect in fibrous composites with piezoelectric and piezomagnetic phases. Physical Review B51 (22), 16424–16427.

Bracke, L.P.M., Van Vliet, R.G., 1981. Broadband magneto-electric transducer using a composite material. International Journal of Electronics 51 (3), 255–262.

Budiansky, B., 1965. On the elastic moduli of some heterogeneous materials. Journal of the Mechanics and Physics of Solids 13 (4), 223–227.

Chan, H.L.W., Unsworth, J., 1989. Simple model for piezoelectric ceramic/polymer 1–3 composites used in ultrasonic transducer applications. IEEE Transactions on Ultrasonics, Ferroelectrics, and Frequency Control 36 (4), 434–441.

Chen, T., 1994. Micromechanical estimates of the overall thermoelectroelastic moduli of multiphase fibrous composites. International Journal of Solids and Structrues 31 (22), 3099–3111.

Christensen, R.M., Lo, K.H., 1979. Solutions for effective shear properties in three phase sphere and cylinder models. Journal of the Mechanics and Physics of Solids 27, 315–330. Errata: 1986. 34 (6), 639.

Christensen, R.M., 1990. A critical evaluation for a class of micromechanics models. Journal of the Mechanics and Physics of Solids 38, 379–404.

Christensen, R.M., 1998. Two theoretical elasticity micromechanics models. Journal of Elasticity 50 (1), 15–25.

Deeg, W.F., 1980. The Analysis of Dislocation, Crack and Inclusion Problems in Piezoelectric Solids. Ph.D. Dissertation, Stanford University.

Dunn, M.L., 1993. Micromechanics of coupled electroelastic composites: effective thermal expansion and pyroelectric coefficients. Journal of Applied Physics 73 (10), 5131–5140.

Dunn, M.L., 1993. Micromechanics of coupled electroelastic composites: effective thermal expansion and pyroelectric coefficients. Journal of Applied Physics 73 (10), 5131–5140.

Dunn, M.L., Taya, M., 1993. Micromechanics predictions of the effective electroelastic moduli of piezoelectric composites. International Journal of Solids and Structrues 30 (2), 161–175.

Eshelby, J.D., 1957. The determination of the elastic field of an ellipsoidal inclusion, and related problems. Proceedings of the Royal Society of London Series A 241, 376–396.

Grekov, A.A., Kramarov, S.O., Kuprienko, A.A., 1989. Effective properties of a transversely isotropic piezocomposite with cylindrical inclusions. Ferroelectrics 99, 115–126.

Hashin, Z., 1962. The elastic moduli of heterogeneous materials. ASME Journal of Applied Mechanics 29 (1), 143–150.

Hashin, Z., Rosen, B.W., 1964. The elastic moduli of fiber-reinforced materials. ASME Journal of Applied Mechanics 31 (2), 223–232. Errata: 1965. 32 (1), 219.

Hill, R., 1965. Theory of mechanical properties of fibre-strengthened materials – III. Self-consistent model. Journal of the Mechanics and Physics of Solids 13 (4), 189–198.

Hori, M., Nemat-Nasser, S., 1998. Universal bounds for effective piezoelectric moduli. Mechanics of Materials 30, 1–19.

Huang, J.H., 1998. Analytical predictions for the magnetoelectric coupling in piezomagnetic materials reinforced by piezoelectric ellipsoidal inclusions. Physical Review B 58 (1), 12–15.

Huang, J.H., Kuo, W.S., 1997. The analysis of piezoelectric/piezomagnetic composite materials containing ellipsoidal inclusions. Journal of Applied Physics 81 (3), 1378–1386.

Jiang, C.P., Cheung, Y.K., 2001. An exact solution for the three-phase piezoelectric cylinder model under antiplane shear and its application to piezoelectric composites. International Journal of Solids and Structrues 38, 4777–4796.

Jiang, C.P., Tong, Z.H., Cheung, Y.K., 2003. A generalized self-consistent method accounting for fiber section shape. International Journal of Solids and Structrues 40, 2589–2609.

Jiang, C.P., Tong, Z.H., Cheung, Y.K., 2001. A generalized self-consistent method for piezoelectric fiber reinforced composites under antiplane shear. Mechanics of Materials 33 (5), 295–308.

Kerner, E.H., 1956. The elastic and thermo-elastic properties of composite media. Proceedings of the Physical Society of London Series B 69, 808–813.

Levin, V., Luchaninov, A., 2001. On the effective properties of thermo-piezoelectric matrix composites. Journal of Physics D: Applied Physics 34, 1–6.

Levin, V.M., Rakovskaja, M.I., Kreher, W.S., 1999. The effective thermoelectroelastic properties of microinhomogeneous materials. International Journal of Solids and Structrues 36, 2683–2705.

Luo, H.A., Weng, G.J., 1987. On Eshelby's inclusions problem in a three-phase spherically concentric solid, and a modification of Mori–Tanaka's method. Mechanics of Materials 6, 347–361.

Mclaughlin, R., 1977. A study of the differential scheme for composite masterials. International Journal of Engineering Science 15 (4), 237–244.

Mori, T., Tanaka, K., 1973. Average stress in matrix and average elastic energy of materials with misfitting inclusions. Acta Metallurgica Sinica 21, 571–574.

Muskhelishivili, N.I., 1965. Some basic problems of mathematical theory of elasticity. Noordhoff, Leyden.

Nan, C.W., 1994. Magnetoelectric effect in composites of piezoelectric and piezomagnetic phases. Physical Review B 50 (9), 6082–6088.

Nan, C.W., 1997. Comment on "The analysis of piezoelectric/piezomagnetic composite materials containing ellipsoidal inclusions" [Journal of Applied Physics 81, 1378 (1997)]. Journal of Applied Physics 82 (10), 5268–5269.

Nemat-Nasser, S., 1999. Micromechanics: Overall Properties of Heterogeneous Materials. Elsevier, Amsterdam.

Ryu, J., Priya, S., Uchino, K., Kim, H.E., 2002. Magnetoelectric effect in composites of magnetostrictive and piezoelectric materials. Journal of Electroceramics 8, 107–119.

Sevostianov, I., Levin, V., Kachanov, M., 2001. On the modeling and design of piezocomposites with prescribed properties. Archive of Applied Mechanics 71, 733–747.

Shaulov, A.A., Smith, W.A., Ting, R.Y., 1989. Modified-lead-titanate/polymer composites for hydrophone applications. Ferroelectrics 93, 177–182.

Smith, J.C., 1974. Correction and extension of van der Pol's method for calculating the shear modulus of a particulate composite. Journal of Research of the National Bureau of Standards 78A (3), 355–362.

Smith, W.A., Shauov, A., 1985. Tailoring the properties of composite piezoelectric materials for medical ultrasonic transducers. IEEE Ultrasonics Symposium 2, 642–647.

Sudak, L.J., 2003. Effect of an interphase layer on the electroelastic stresses within a three-phase elliptic inclusion. International Journal of Engineering Science 41, 1019–1039.

Tadmor, E.B., Philips, R., Ortiz, M., 2000. Hierarchical modeling in the mechanics of materials. International Journal of Solids and Structrues 37, 379–389.

Van Run, A.M.J.G., Terrell, D.R., Scholing, J.H., 1974. An in situ grown eutectic magnetoelectric composite materials. Part 2: physical properties. Journal of Materials Science 9, 1710–1714.

Van Suchtelen, J., 1972. Product properties: a new application of composite materials. Philips Research Reports 27, 28–37.

Wang, B., 1992. Three-dimensional analysis of an ellipsoidal inclusion in a piezoelectric material. International Journal of Solids and Structrues 29, 293–308.